# Influence of planar and point defects on the basal-plane conductivity of HoBaCuO single crystals

Vovk, R.V. , Khadzhai, G.Y. , Dobrovolskiy, O.V. , Nazyrov, Z.F. and Chroneos, A.

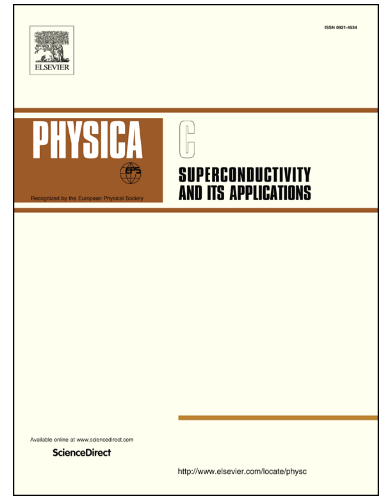


# Influence of planar and point defects on the basal-plane conductivity of HoBaCuO single crystals


Ruslan V. Vovk, Georgij Ya. Khadzhai, Oleksandr V. Dobrovolskiy, Zarif F. Nazyrov, Alexander Chroneos



PII: S0921-4534(15)00214-2
DOI: http://dx.doi.org/10.1016/j.physc.2015.06.011
Reference: PHYSC 1252880

To appear in: *Physica C*

Received Date: 21 May 2015
Accepted Date: 18 June 2015

# Influence of planar and point defects on the basal-plane conductivity of HoBaCuO single crystals

Ruslan V. Vovk[a], Georgij Ya. Khadzhai[a], Oleksandr V. Dobrovolskiy[a,b], Zarif F. Nazyrov[a], Alexander Chroneos[c]

[a]*Physics Department, V. Karazin Kharkiv National University, Svobody Sq. 4, 61077 Kharkiv, Ukraine*
[b]*Physikalisches Institut, Goethe University, Max-von-Laue-Str. 1, 60438 Frankfurt am Main, Germany*
[c]*Faculty of Engineering and Computing, Coventry University, UK*

**Abstract**

The resistivity along and across twin boundaries in $HoBa_2Cu_3O_{7-\delta}$ single crystals is investigated in the temperature range $T_c$−300 K. It is revealed that the twin boundaries enhance inhomogeneity of the oxygen distribution, whereby regions near them are depleted in oxygen. The normal-state conductivity is determined by scattering of electrons on phonons and defects both along and across the twin boundaries. Near $T_c$, the electrical conductivity can be described within the framework of the 3D Aslamazov-Larkin fluctuation model. It is found that the twin boundaries increase the intensity of the electron-phonon scattering and reduce the transverse coherence length $\xi_c(0)$.

*Keywords:* superconducting cuprates, transverse resistance, praseodymium anomaly, electrical resistance measurements

## 1. Introduction

As is known, identification of the charge carriers scattering mechanisms is important for conceiving the nature of non-trivial phenomena exhibited by high-temperature superconductors (HTSCs) in the normal state [1, 2]. To these phenomena are related the pseudogap [3–5] and fluctuation [6–8] anomalies, the metal-to-insulator transition [9, 10], the incoherent electronic transport [11, 12] and so forth. According to contemporary views [1–5], it is these phenomena which may serve as a key to understanding the microscopic mechanism of HTSC, which remains unsettled despite the 29 year-long record of intensive experimental and theoretical research.

When studying the aforementioned phenomena, compounds from the so-called 1-2-3 system ($YBa_2Cu_3O_{7-\delta}$) are most asked-for. This is stipulated by their relative high ($\approx$ 90 K) superconducting transition temperature $T_c$ [13], above the nitrogen liquefaction temperature, and a relative simplicity of changing their physical characteristics by varying the oxygen content [14, 15] as well as a full [16] or a partial [17, 18] substitution of other constituents.

As it has been believed until recently, substituting Y for other rare earths [16, 19], with exception of Pr (Pr anomaly) [1, 20, 21], does not substantially affect the conducting properties of the system ReBaCuO (Re=Y or lanthanides). However, as it has been revealed in recent works [22, 23], substitution of Y for Ho in the case of oxygen-nonstoichiometric samples may notably affect the ordering processes in the oxygen subsystem and stimulate the appearance of specific diffusion mechanisms such as, e. g., the ascending diffusion [23].

At the same time, the role of a series of additional factors remains unsettled, such as twin boundaries (TBs) [24, 25] and phase inclusions differing by the oxygen content and, hence, having different conducting characteristics [26, 27]. TBs always appear in HTSC compounds from the 1-2-3 system in consequence of the ferroelastic tetra-ortho transition in the course of saturation of samples with oxygen [28, 29]. TBs are an additional source of anisotropy [30] along with the conventional structural anisotropy [31]. Phase inclusions appear as a result of reordering of the labile component [32–34] and may built specific superstructural formations in the system [35–37]. Both these factors significantly expand the research field and are of interest from both, applications-related and basic research viewpoints.

Given the motivation above, here we investigate the basal-plane conductivity in $HoBa_2Cu_3O_{7-\delta}$ single crystals for different geometries of the transport current with respect to TBs and, in particular, focus on the optimally-oxygen-doped (before annealing) and the reduced-oxygen-content (after annealing) states.

## 2. Experimental

The $HoBa_2Cu_3O_{7-\delta}$ single crystals were grown by the solution-melt technique in a gold crucible according to the growth protocol similar to that used for $YBa_2Cu_3O_{7-\delta}$ [18]. For electrical resistance measurements, several single-crystals were selected from one growth series, with the following dimensions: $2 \times 1.8 \times 0.5\,\mathrm{mm}^3$ (K1) and $1.9 \times 1.9 \times 0.5\,\mathrm{mm}^3$ (K2) (the smallest size corresponds to the $c$-axis). These crystals were used for the preparation of samples differing by the direction of TBs with regard to the transport current direction in the $ab$-plane, namely the transport current vector $\mathbf{I}$ || TBs for

*Corresponding author
*Email address:* Dobrovolskiy@Physik.uni-frankfurt.de (Oleksandr V. Dobrovolskiy)

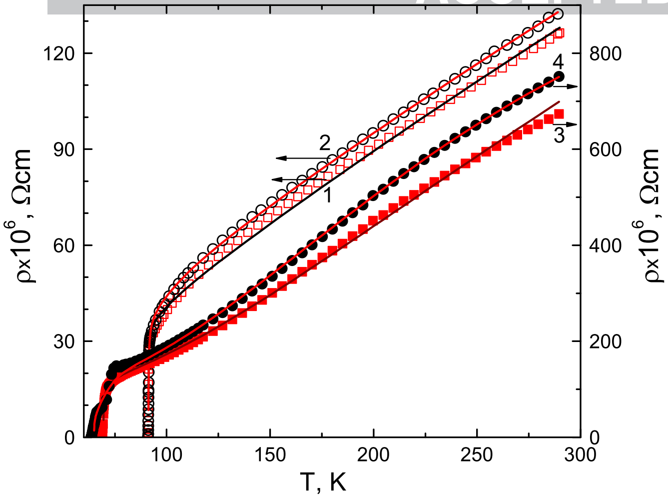


Figure 1: Temperature dependences of the resistivity of the $HoBa_2Cu_3O_{7-\delta}$ single crystals. Open symbols – before annealing: 1 – along TBs, 2 – across TBs. Solid symbols – after annealing: 3 – along TBs, 4 – across TBs. Symbols: experiment; lines – fits to Eqs. (1)–(2).

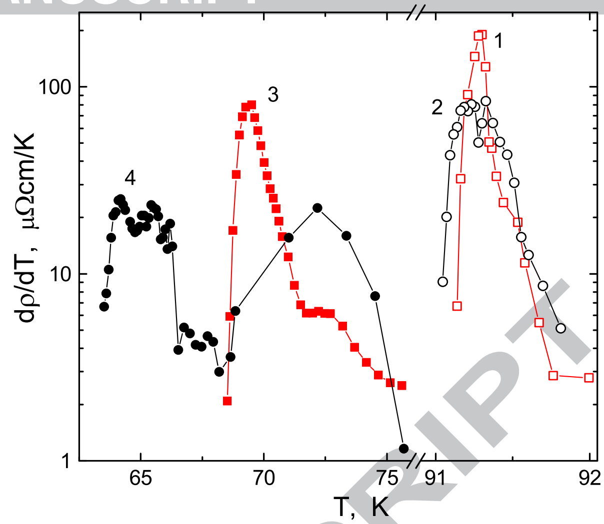


Figure 2: Derivatives $d\rho/dT$ in the superconducting transition area. Designations are the same as in Fig. 1.

K1 and **I** is tilted at 45° to TBs for K2. The electrical contacts were formed by gluing gold conductors of 0.05 mm diameter with a silver paste, that allowed one to obtain a contact transient resistance of less than 1 Ω. The electrical resistance in the basal plane and along the *c*-axis was measured with a dc current up to 10 mA. To obtain samples with the optimal oxygen content and a high $T_c$, they were annealed in an oxygen flow at 420°C for three days. For reducing the oxygen content the samples were annealed in air at 500°C. The measurements were done in the temperature-sweep mode, in 3 days after annealing that ensured an equilibrium oxygen distribution over the sample volume at room temperature [7].

## 3. Results and discussion

Figure 1 presents the temperature dependences of the resistivity along and across TBs prior to (curves 1 and 2) and after (curves 3 and 4) annealing. One sees that in both cases $\rho(T)$ across TBs is larger than $\rho(T)$ along TBs. Still, the curves $\rho(T)$ along and across TBs differ not so much, especially in the optimally-oxygen-doped state. This allows one to conclude that the influence of TBs on the resistance of $HoBa_2Cu_3O_{7-\delta}$ is relatively weak.

Figure 2 depicts the derivatives $d\rho/dT$ in the vicinity of the superconducting transition. One sees that even before annealing, the oxygen distribution is nonuniform in the sample. This is reflected in the that the maxima in the derivatives (curves 1 and 2) are asymmetric and the maxima in $d\rho/dT$ across TBs are notably broader than along TBs. The latter signature suggests that TBs enhance the nonuniformity of the oxygen distribution. Annealing in air at 500°C leads to the increase of the oxygen deficit to 0.18 [38] and thereby enhances the nonuniformity of the oxygen distribution in the sample. Thus, in measurements along TBs after annealing, the asymmetry of the maximum in $d\rho/dT$ has increased, resulting in a "shoulder" in the range close to 72 K (curve 3). Across TBs two maxima in $d\rho/dT$ have appeared in the ranges near 72 K and 65 K (curve 4) that points to the presence of phases with the respective $T_c$ in the sample [39].

Note that the shape of the derivatives $d\rho/dT$ in the vicinity of the superconducting transition is rather sensitive to the inhomogeneity of the sample. Hence, an analysis of the derivatives allows one to draw conclusions about the sample structure, see e.g. [26]. Namely, since the phase with $T_c \approx 72$ K becomes apparent in both geometries ("shoulder" in the vicinity of 72 K), it likely is not related to TBs. The phase with $T_c \approx 65$ K is only revealed in measurements across TBs and has minimal $T_c$, that is zero resistance is attained in this phase. This phase is likely localized near TBs and has a mostly strong oxygen deficit. In other words, regions near TBs have a reduced oxygen content. The phase with $T_c \approx 69$ K manifests itself only in measurements along TBs. The zero-resistance state attained in this phase suggests the presence of percolation paths along TBs over this phase. The latter is possible provided this phase has a filament structure along TBs or the conductivity proceeds in the twin plane.

The temperature dependences of the resistance of the single crystals, in the range $T_c$ to 300 K, we approximated to an expression accounting for electron scattering on phonons and defects [40], as well as the fluctuation conductivity within the framework of the 3D Aslamazov-Larkin model [41]. The general expression for the conductivity reads

$$\sigma = \rho_n^{-1} + \Delta\sigma_{AL}, \qquad \rho_n = (\rho_0 + \rho_{ph})(1 + b_0 T^2),$$

$$\rho_{ph}(T) = \tilde{C}_3 (\frac{T}{\theta})^3 \int_0^{\theta/T} \frac{x^3 dx}{(e^x - 1)^2} + \qquad (1)$$

$$C_5 (\frac{T}{\theta})^5 \int_0^{\theta/T} \frac{x^5 dx}{(e^x - 1)^2}.$$

Here $\rho_0$ is the residual resistivity characterizing scattering on defects, in $\rho_{ph}(T)$ the first term describes the contribution to the resistivity owing to the interband scattering of electrons on phonons, the second term accounts for the intraband scattering, $\theta$ is the Debye temperature, $b_0$ depends on the shape of the density of electronic states curve, the effective mass of the charge carriers and the Fermi energy [42, 43]. The fluctuation conductivity reads

$$\Delta\sigma_{AL} = \frac{e^2}{16\hbar\xi_c(0)\sqrt{2\varepsilon_0}\sinh(2\varepsilon/\varepsilon_0)}. \quad (2)$$

This expression for the fluctuation conductivity is chosen for limiting the range of its contribution [44], $\varepsilon = \ln(T/T_c)$ is the reduced temperature, $T_c$ is the transition temperature in the mean-field approximation $T > T_c$, $\xi_c$ is the transverse coherence length, $\varepsilon_0$ determines the temperature interval of superconducting fluctuations $\varepsilon_0 = \ln(T_{fluct}/T_c)$, $T_{fluct}$ is the characteristic temperature above which superconducting fluctuations are absent.

Note that according to [26], the appearance of fluctuational Cooper pairs above $T_c$ causes a decrease of the one-electron density of states at the Fermi level, that is leads to the appearance of the pseudogap at $T \approx T_{fluct}$. However, accounting for the corresponding change of the normal resistance is complicated, since it is masked by a much stronger singular fluctuation conductivity which determines the run of $\rho(T)$ near $T_c$.

The optimal set of fitting parameters is compiled in Table 1. It allows one approximate the experimental data in the whole temperature range $T_c$ to 300 K with an error of about 3%. Also, the derivatives calculated by using Eq. (1) adequately describe the behavior of $d\rho/dT$ derived from the experimental data in the whole temperature range. The fits are shown in Fig. 1 by solid lines.

| State | before annealing | | after annealing | |
|---|---|---|---|---|
| Parameters | along TBs | across TBs | along TBs | across TBs |
| $T_c$, K | 91.3 | 91.3 | 69.5 | 64.9 |
| $\rho_0$, $\mu\Omega$cm | 15.15 | 20.5 | 120 | 94 |
| $C_3$, $\mu\Omega$cm | 277 | 280 | 2900 | 3940 |
| $C_5$, $\mu\Omega$cm | 0 | 0 | 1100 | 1320 |
| $\theta$, K | 331 | 331 | 662 | 665 |
| $b_0 \times 10^6$, K$^{-2}$ | −0.2 | −0.31 | −0.25 | −1.99 |
| $\xi_c(0)$, Å | 1.4 | 0.9 | 1.6 | 0.4 |
| $\Delta T = T_{fluct} - T_c$, K | 8.6 | 9.6 | 30 | 3.7 |

Table 1: Parameters of the superconducting transition for three aging terms.

In Table 1 one sees that in the initial, optimally-oxygen-doped state (before annealing) the superconducting transition temperatures $T_c$ as well as the parameters $C_3$, $C_5$ and $\theta$ for both geometries along and across TBs are the same. At the same time $\rho_0^{along} < \rho_0^{across}$ and $\xi_c^{along} > \xi_c^{across}$. In this way, the influence of TBs on the resistance of the optimally doped $HoBa_2Cu_3O_{7-\delta}$ becomes apparent only at low temperatures as $\rho_0 = \rho(T \to 0)$. Namely, TBs somewhat raise the residual resistivity $\rho_0$ and reduce the transverse coherence length $\xi_c(0)$.

No effect of TBs on $T_c$ and $\theta$, which determine the electron-phonon interaction, has been observed in both, before- and after-500°C-annealing measurements. The fact that $\xi_c^{along}(0) > \xi_c^{across}(0)$ can be explained by a decrease of the Fermi velocity $v_F$ owing to TBs.

The 500°C-annealing has caused an about two-fold increase of $\theta$. A similar behavior of the Debye temperature with increasing oxygen deficit was observed in [45] and attributed to an enhancement of the interatomic interaction. Note that after the 500°C-annealing, which has led to a substantial variation of the $\rho(T)$ fitting parameters in Table 1, these relate to some effective medium rather than to a well-defined phase. Nevertheless, since the variations in $T_c$ are not large, the differences in the transport properties of these phase may be regarded as minor.

After annealing, $\rho_0$ has increased by several factors for both geometries, whereby $\rho_0^{along} > \rho_0^{across}$. This relation between $\rho_0^{along}$ and $\rho_0^{across}$ may be stipulated by the sample inhomogeneity, in particular, by the shape anisotropy of the phase formations and scattering at the phase boundaries. An abrupt rise of the parameter $b_0^{across}$ in comparison with its other values may also be caused by the sample inhomogeneity.

The parameter $C_3$ has risen by an order of magnitude for both geometries, whereby $C_3^{along} < C_3^{across}$. For fitting the $\rho(T)$ curve after annealing it was necessary to introduce the parameter $C_5$, for which again $C_5^{along} < C_5^{across}$. These relations between the values of $C_3$ and $C_5$ attest to an increase of the intensity of electron scattering on phonons near TBs. A certain role at this can be played by other specific mechanisms of the quasiparticle scattering [46–50].

## 4. Conclusions

In summary, the study of the temperature dependence of the resistance of $HoBa_2Cu_3O_{7-\delta}$ along and across twin boundaries (TBs) has revealed that (i) the influence of TBs on the resistance is rather weak, (ii) TBs enhance the inhomogeneity of the oxygen distribution, and (iii) areas near TBs have a reduced oxygen content. The temperature dependences of the resistance of the single crystals in the range $T_c$ to 300 K, for both geometries along and across TBs, can be presented as a result of electron scattering on phonons and defects in conjunction with the fluctuation conductivity near $T_c$. At the same time, no influence of TBs on $T_c$ and the Debye temperature has been revealed. TBs increase the intensity of electron scattering by phonons and reduce the coherence length $\xi_c(0)$.

## References


[1] J. Ashkenazi, J. Supercond. Nov. Magnet. 24 (4) (2011) 1281–1308.

[2] R. V. Vovk, G. Y. Khadzhai, O. V. Dobrovolskiy, Appl. Phys. A 117 (2014) 9971002.

[3] M. V. Sadovskii, I. A. Nekrasov, E. Z. Kuchinskii, T. Pruschke, V. I. Anisimov, Phys. Rev. B 72 (2005) 155105.

[4] A. Solovjov, M. Tkachenko, R. Vovk, A. Chroneos, Physica C 501 (0) (2014) 24 – 31.

[5] R. V. Vovk, G. Y. Khadzhai, O. V. Dobrovolskiy, Solid State Commun. 204 (0) (2015) 64 – 66.

[6] T. A. Friedmann, J. P. Rice, J. Giapintzakis, D. M. Ginsberg, Phys. Rev. B 39 (1989) 4258–4266.

[7] R. V. Vovk, N. R. Vovk, G. Y. Khadzhai, O. V. Dobrovolskiy, Z. F. Nazyrov, Curr. Appl. Phys. 14 (12) (2014) 1779 – 1782.
[8] R. Vovk, G. Khadzhai, I. Goulatis, A. Chroneos, Physica B 436 (0) (2014) 88 – 90.
[9] K. Widder, D. Berner, H. Geserich, W. Widder, H. Braun, Physica C 251 (3–4) (1995) 274 – 278.
[10] R. V. Vovk, Z. F. Nazyrov, I. L. Goulatis, A. Chroneos, Physica C 485 (2013) 89–91.
[11] P. W. Anderson, Phys. Rev. Lett. 67 (1991) 2092–2094.
[12] R. V. Vovk, M. A. Obolenskii, A. A. Zavgorodniy, I. L. Goulatis, A. I. Chroneos, V. M. Pinto Simoes, J. Mater. Sci.: Mater. Electron. 20 (9) (2009) 858–860.
[13] M. K. Wu, J. R. Ashburn, C. J. Torng, P. H. Hor, R. L. Meng, L. Gao, Z. J. Huang, Y. Q. Wang, C. W. Chu, Phys. Rev. Lett. 58 (1987) 908–910.
[14] R. Beyers, B. T. Ahn, G. Gorman, V. Y. Lee, S. S. P. Parkin, M. L. Ramirez, K. P. Roche, J. E. Vazquez, T. M. Gur, R. A. Huggins, Nature 340 (1989) 619–621.
[15] M. A. Obolenskii, R. V. Vovk, A. V. Bondarenko, N. N. Chebotaev, Low Temp. Phys. 32 (6) (2006) 571–575.
[16] D. M. Ginsberg (Ed.), Physical properties of high temperature superconductors I., Word Scientific, Singapore, 1989.
[17] A. Chroneos, I. L. Goulatis, R. V. Vovk, Acta Chim. Sloven. 54 (2007) 179.
[18] R. V. Vovk, N. R. Vovk, O. V. Shekhovtsov, I. L. Goulatis, A. Chroneos, Supercond. Sci. Technol. 26 (8) (2013) 085017–1–8.
[19] Y. Yan, M. Blanchin, G. Fuchs, J. Less Comm. Met. 164–165 (0) (1990) 215 – 222.
[20] M. Akhavan, Physica B 321 (1–4) (2002) 265–282.
[21] R. Vovk, N. Vovk, G. Khadzhai, I. Goulatis, A. Chroneos, Sol. State Commun. 190 (0) (2014) 18 – 22.
[22] R. V. Vovk, M. A. Obolenskii, A. A. Zavgorodniy, I. L. Goulatis, V. I. Beletskii, A. Chroneos, Physica C 469 (5–6) (2009) 203–206.
[23] R. V. Vovk, Z. F. Nazyrov, M. A. Obolenskii, I. L. Goulatis, A. Chroneos, V. M. Pinto Simoes, Philos. Mag. 91 (17) (2011) 2291–2302.
[24] M. Sarikaya, R. Kikuchi, A. I. A., Physica C 152 (2) (1988) 161 – 170.
[25] R. V. Vovk, M. A. Obolenskii, A. A. Zavgorodniy, Z. F. Nazyrov, I. L. Goulatis, V. V. Kruglyak, A. Chroneos, Mod. Phys. Lett. B 25 (2011) 2131–2136.
[26] R. M. Costa, F. T. Dias, P. Pureur, X. Obradors, Physica C 495 (0) (2013) 202 – 207.
[27] R. V. Vovk, N. R. Vovk, O. V. Dobrovolskiy, J. Low Temp. Phys. 175 (3-4) (2014) 614–630.
[28] G. Lacayo, G. Kästner, R. Herrmann, Physica C 192 (1-2) (1992) 207–214.
[29] R. V. Vovk, M. A. Obolenskii, Z. F. Nazyrov, I. L. Goulatis, A. Chroneos, V. M. Pinto Simoes, J. Mater. Sci. - Mater. Electron. 23 (6) (2012) 1255–1259.
[30] A. V. Bondarenko, A. A. Prodan, M. A. Obolenskii, R. V. Vovk, T. R. Arouri, Low Temp. Phys. 27 (5) (2001) 339–344.
[31] R. V. Vovk, G. Y. Khadzhai, O. V. Dobrovolskiy, Mod. Phys. Lett. B 28 (17) (2014) 1450142.
[32] J. D. Jorgensen, S. Pei, P. Lightfoor, H. Shi, A. P. Paulikas, B. W. Veal, Physica C 167 (5-6) (1990) 571–578.
[33] J. Kircher, M. Cardona, A. Zibold, K. Widder, H. P. Geserich, Phys. Rev. B 48 (1993) 9684–9688.
[34] D. D. Balla, A. V. Bondarenko, R. V. Vovk, M. A. Obolenskii, A. A. Prodan, Low Temp. Phys. 23 (10) (1997) 777–781.
[35] H. Lütgemeier, S. Schmenn, P. Meuffels, O. Storz, R. Schöllhorn, C. Niedermayer, I. Heinmaa, Y. Baikov, Physica C 267 (3–4) (1996) 191 – 203.
[36] T. Krekels, H. Zou, G. V. Tendeloo, D. Wagener, M. Buchgeister, S. Hosseini, P. Herzog, Physica C 196 (1992) 363–368.
[37] R. Vovk, N. Vovk, A. Samoilov, I. Goulatis, A. Chroneos, Sol. State Comm. 170 (0) (2013) 6–9.
[38] W. Wong-Ng, L. P. Cook, H. B. Su, M. D. Vaudin, C. K. Chiang, D. R. Welch, E. R. Fuller, J. Z. Yang, L. H. Bennett, J. Res. Natl. Inst. Stand. Technol. 111 (2006) 41–55.
[39] V. I. Simonov, V. N. Molchanov, B. K. Vanstein, JETP Lett. 46 (1987) 199–201.
[40] L. Colquitt, J. Appl. Phys. 36 (8) (1965) 2454–2458.
[41] L. G. Aslamazov, A. I. Larkin, Fiz. Tverd. Tela 10 (1968) 1104.
[42] T. Aisaka, M. Shimizu, J. Phys. Soc. Jap. 28 (3) (1970) 646–654.
[43] E. A. Zhurakovskiy, V. F. Nemchenko, Cinetic properties and electronic structure of interstitials, Naukova dumka, Kiev, 1989.
[44] B. Leridon, A. Défossez, J. Dumont, J. Lesueur, J. P. Contour, Phys. Rev. Lett. 87 (2001) 197007.
[45] R. Vovk, G. Khadzhai, O. Dobrovolskiy, N. Vovk, Z. Nazyrov, J. Mater. Sci: Mater. Electron. 26 (3) (2015) 1435–1440.
[46] D. H. S. Smith, R. V. Vovk, C. D. H. Williams, A. F. G. Wyatt, Phys. Rev. B 72 (2005) 054506.
[47] D. H. S. Smith, R. V. Vovk, C. D. H. Williams, A. F. G. Wyatt, New J. Phys. 8 (8) (2006) 128–1–8.
[48] I. N. Adamenko, K. E. Nemchenko, V. I. Tsyganok, A. I. Chervanev, Low Temp. Phys. 20 (7) (1994) 498–504.
[49] V. M. Apalkov, M. E. Portnoi, Phys. Rev. B 65 (2002) 125310.
[50] P. J. Curran, V. V. Khotkevych, S. J. Bending, A. S. Gibbs, S. L. Lee, A. P. Mackenzie, Phys. Rev. B 84 (2011) 104507.

highlights

The resistance of HoBaCuO single crystals is investigated

Electron-phonon scattering and fluctuation terms are quantified

Twin boundaries are found to reduce the transverse coherence length